Exchange bias in La0.7Sr0.3MnO3/NiO and LaMnO3/NiO interfaces

X. K. Ning, Z. J. Wang, X. G. Zhao, C. W. Shih, and Z. D. Zhang

Citation: J. Appl. Phys. **113**, 223903 (2013); doi: 10.1063/1.4811227
View online: http://dx.doi.org/10.1063/1.4811227
View Table of Contents: http://jap.aip.org/resource/1/JAPIAU/v113/i22
Published by the AIP Publishing LLC.

Exchange bias in $La_{0.7}Sr_{0.3}MnO_3$/NiO and $LaMnO_3$/NiO interfaces

X. K. Ning,[1] Z. J. Wang,[1,a)] X. G. Zhao,[1,2] C. W. Shih,[2] and Z. D. Zhang[1]
[1]*Shenyang National Laboratory for Materials Science, Institute of Metal Research, Chinese Academy of Sciences, 72 Wenhua Road, Shenyang 110016, China*
[2]*Department of Physics, National Chung Cheng University, Chia-Yi 62102, Taiwan*

(Received 10 April 2013; accepted 30 May 2013; published online 13 June 2013)

Bilayers of $La_{0.7}Sr_{0.3}MnO_3$/NiO and $LaMnO_3$/NiO were prepared and magnetic exchange coupling investigated in these bilayers, where the Curie temperature of the ferromagnetic (FM) layer is lower than the Néel temperature of the antiferromagnetic layer. After small-field cooling, the LSMO/NiO bilayer exhibits an exchange bias with field $H_{EB} = 60$ Oe, whereas the LMO/NiO sample shows weak magnetic interaction (~22 Oe). The unconventional exchange bias in LSMO/NiO bilayer vanishes as temperature rises above 50 K. The weak magnetic interaction at the LMO/NiO interface is due to a larger Hubbard parameter value and smaller transfer integral value in the Mott insulator LMO compared with that for the FM conductor LSMO. The valence states of Mn and Ni ions across the interfaces for LSMO/NiO and LMO/NiO have been studied using X-ray photoelectron spectroscopy. We speculate that the FM interaction between Ni^{2+} and Mn^{4+} gives rise to magnetic regions that pin the ferromagnetic LSMO layer. © *2013 AIP Publishing LLC*. [http://dx.doi.org/10.1063/1.4811227]

I. INTRODUCTION

Exchange bias (EB) has been widely studied in various magnetic systems for both its theoretical significance and potential applications in magnetic recording media, spin valves, and magnetic tunnel junction, since it was first discovered in ferromagnetic (FM) Co particles covered by antiferromagnetic (AF) CoO.[1–4] Recently, remarkable improvement in techniques for growing and characterizing oxide thin films has allowed a renewed interest in the EB effect at the interface of ABO_3 perovskite oxide structures. In these systems, there have been many interesting experimental results on the EB effect, such as positive EB in the $La_{0.7}Sr_{0.3}MnO_3$ (LSMO)/$SrRuO_3$ bilayer, unexpected EB in FM/Pauli paramagnetic (PM) and FM/diamagnetic (DM) systems, and unconventional EB in systems where the Curie temperature T_C of the FM layer is lower than the Néel temperature T_N of the AF layer.[5–10] The EB effect can be influenced by various factors, including uncompensated magnetic moment, interfacial charge transfer, and magnetic structure change at the interface. Among these structures, LSMO and $LaMnO_3$ (LMO) with $T_C \approx 340$ K and 150 K, respectively, have always been selected as the FM layer. Bulk stoichiometric LMO is a Mott insulator with a large Hubbard parameter U and an A-type AF ordering. However, when grown as a thin film, LMO exhibits FM insulator properties,[8,11] whereas LSMO is a double-exchange FM conductor and shows different d-p hybridization.[12] Interestingly, in comparing the exchange coupling between the LSMO/AF and LMO/AF bilayers with the same AF layer, one would expect that the interfacial coupling is different in these two bilayers, even if both LSMO and LMO have high density e_g electron and magnetic moment.[13]

In this paper, we report experimental results on the EB effect in both LSMO/NiO and LMO/NiO bilayers epitaxially grown on normal $SrTiO_3$ (STO) substrates. After small-field cooling starting from 340 K (lower than the T_N of NiO), a distinct EB effect is observed in the LSMO/NiO structure, whereas interfacial coupling is weak across the LMO/NiO interface. The difference in the EB effect for these bilayers will be discussed.

II. EXPERIMENTAL PROCEDURE

LMO and LSMO thin films were both grown on STO (001) single-crystal substrates (with a cubic lattice and the lattice parameter a = 0.391 nm) by pulsed laser deposition (PLD) using a KrF ($\lambda = 248$ nm) excimer laser. The laser flux is approximately 1.4 J/cm^2 with a repetition rate of 2 Hz. Initially, LSMO or LMO was deposited on a STO substrate at 0.5-mbar pressure of pure O_2 at a substrate temperature of 700 °C, and then NiO films were deposited on the LSMO or LMO layer using a sintered NiO target at 550 °C. The samples were finally annealed at a pressure of 0.5 bar of pure O_2 to remove oxygen vacancies. Both LSMO(10 nm)/NiO(20 nm) and LMO(10 nm)/NiO(20 nm) bilayers were grown under the same conditions. Structural quality and lattice parameters of the thin films were analyzed by X-ray diffraction (XRD) (Rigaku, D/max-2000, CuK_α radiation). Surface morphology was characterized by atomic force microscopy (AFM). Microstructure and thickness of the films were obtained from transmission electron microscopy (TEM) (F20, Tecnai). Epitaxy between the films and substrate was also confirmed by high-resolution TEM (HRTEM). The chemical states of the elements in the films were determined by X-ray photoelectron spectroscopy (XPS), (Therma ESCALAB 250; Al Kα source, 1486.60 eV, Resolution: 400 meV, Energy step: 0.1 eV), and the binding energies of the different peaks were calibrated using the C_{1s}

a)Author to whom correspondence should be addressed. Electronic mail: wangzj@imr.ac.cn

photoelectron binging energy of 285.0 eV. Magnetization measurements were performed from 5 to 340 K and external magnetic fields up to 3 kOe using a superconducting quantum interference device magnetometer.

III. RESULTS AND DISCUSSION

The XRD spectra of the LSMO/NiO and LMO/NiO bilayers on the STO (001) substrate (Fig. 1(a)) indicate that the LSMO and LMO films are epitaxially grown on the STO surface. Highly (100) textured LSMO and LMO films were obtained. Only the (200) peak of NiO can be observed from the XRD data, indicating that NiO is also epitaxially grown on the LSMO and LMO layers; meanwhile, no secondary phases such as Ni_2O and Ni_2O_3 exist in the NiO layer.

Typical AFM surface morphologies of these films ($2 \times 2\,\mu$m) are shown in Fig. 1(b). The surfaces of both LSMO/NiO and LMO/NiO bilayers are very smooth with a roughness of 0.9 nm and 0.5 nm, respectively, suggesting a flat surface and high quality of epitaxial NiO thin film on top of the perovskite structure. The high crystalline quality of the bilayers can also be confirmed by cross-sectional TEM images. For example, the interface between the LSMO and NiO (Fig. 2) is clear and flat with a film thickness of 10 and 20 nm, respectively. A HRTEM image (Fig. 2(b)) also reveals a clear and well-defined film/film interface (marked by a dashed arrow) in which it is possible to see that both the LSMO and NiO films have grown epitaxially on the STO substrate.

Figure 3 presents the temperature dependence of magnetization for both LSMO/NiO and LMO/NiO bilayers with an in-plane magnetic field $H = 100$ Oe applied. For both systems, magnetization decreases with increasing temperature, and a FM-to-PM transition is observed. The FM behavior of the LMO is in line with recent experimental reports,[14,15] and the T_C value is in good agreement with the reported values (120–200 K) in LMO thin films grown by PLD.[11] The transition temperature is determined to be 330 K and 150 K for

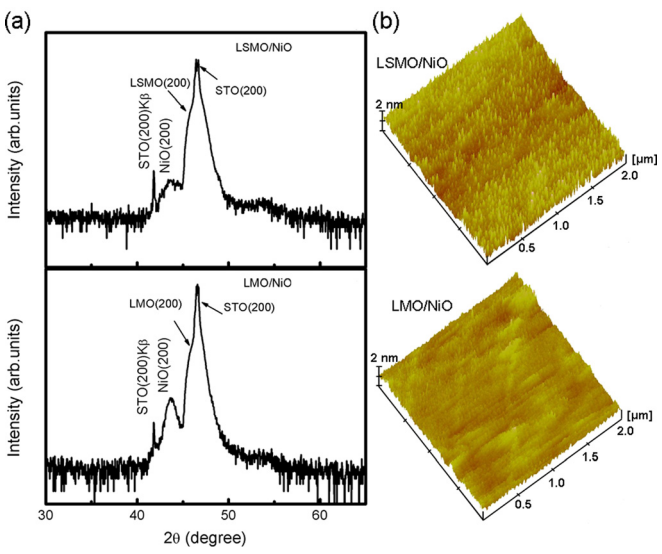

FIG. 1. (a) XRD spectra of LSMO/NiO and LMO/NiO bilayers. (b) Surface AFM images of LSMO/NiO and LMO/NiO bilayers.

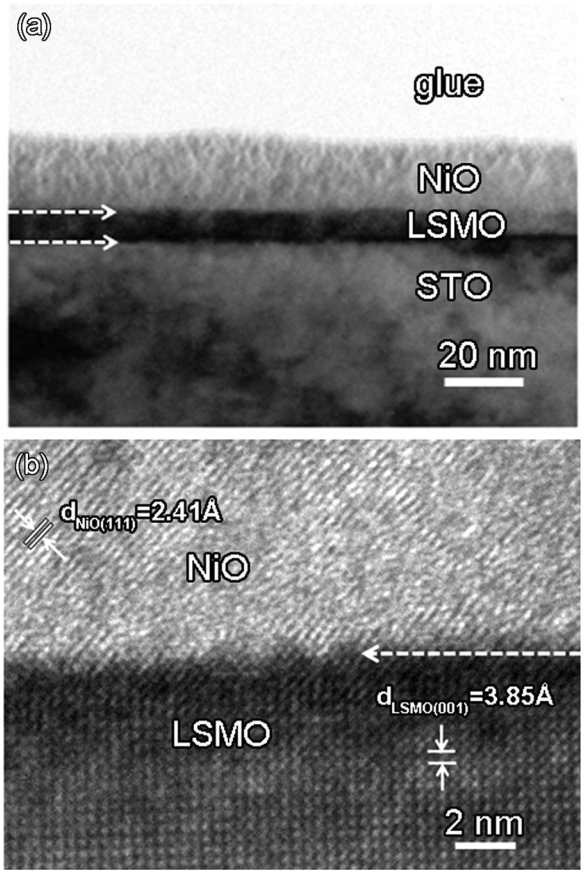

FIG. 2. (a) A low-magnification TEM micrograph of cross-sectional LSMO(10 nm)/NiO(20 nm) bilayer. (b) A High-resolution TEM image of LSMO/NiO bilayer.

LSMO and LMO phases, respectively, and these values are far below the T_N of NiO.[16]

Magnetic hysteresis loops were obtained at 5 K after field cooling (FC), performed in a magnetic field of ±3 kOe from 340 K (above T_C but below T_N). For comparison, magnetization loops of the LSMO/NiO (Fig. 4(a)) and LMO/NiO (Fig. 4(b)) after zero-field cooling (ZFC) are also shown. Magnetic fields above ±1300 Oe are applied to attain saturated magnetization M_s. From Fig. 4, the LSMO/NiO bilayer shows a saturated magnetization of 507 emu/cm^3 (3.26 μ_B/Mn)

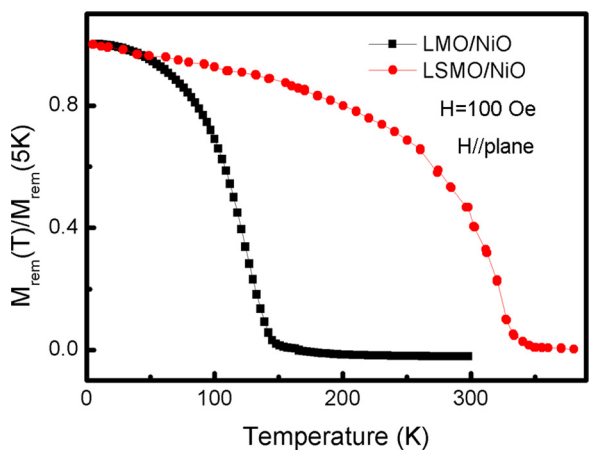

FIG. 3. Temperature dependence of magnetization of LSMO/NiO and LMO/NiO bilayers under an in-plane magnetic field of 100 Oe.

in contrast to 227 emu/cm^3 (1.45 μ_B/Mn) in the LMO/NiO bilayer, implying a conversion from Mn^{3+} to Mn^{4+} in the LMO film.[17] The hysteresis loops are clearly seen to be shifted along the magnetic-field axis, indicating that the EB effect exists in these samples. The absolute values of the EB field H_{EB} and of coercivity H_C are calculated using $H_{EB} = |H_1 + H_2|/2$ and $H_C = |H_1 - H_2|/2$, where H_1 and H_2 are the values of magnetic field at which the magnetization goes to zero. A large H_{EB} of about 60 Oe is observed in the LSMO/NiO bilayer. When switching the field both during FC and in hysteresis loops measurement from in-plane to out-of-plane, we obtain a similar magnitude for the EB field (~76 Oe) (see inset of Fig. 4(a)). The shift of the hysteresis loops is found to be highly reversible with respect to the field direction during FC, i.e., $H_{EB} \sim -60$ Oe and $H_{EB} \sim 72$ Oe, corresponds to +3000 Oe and −3000 Oe, respectively. More importantly, this H_{EB} value is much larger than that of the EB field (~22 Oe) in the LMO/NiO bilayer. Moreover, we found a strong sensitivity of H_C and H_{EB} to FC. A strong enhancement of the coercivity H_C and H_{EB} after FC (H = ±3000 Oe) compared with ZFC is obtained. The EB field of these samples after ZFC from 340 K is zero within the 10-Oe measurement resolution.

All the ZFC magnetization loops are narrower than the FC loops. This is in line with the conventional EB observed in FM/AFM structures.[18] It is, indeed, found experimentally that the uncompensated spins pinned at the interface should play an important role for the EB effect in the LSMO/NiO and LMO/NiO bilayers. This is similar to the results in the $BiFeO_3$-based films.[10,19] Cai *et al.* reported that for $T_C < T_N$, the magnetic coupling has been established when the FM layer is in the PM state.[20] In their experiment, through applying a magnetic field at temperatures above T_C but below T_N, they found uncompensated spins are induced and coupled to the FM layer.[21–23] By analogy, uncompensated spins pinned at the interface should play a similarly important role in the EB effect for our LSMO/NiO and LMO/NiO bilayers.

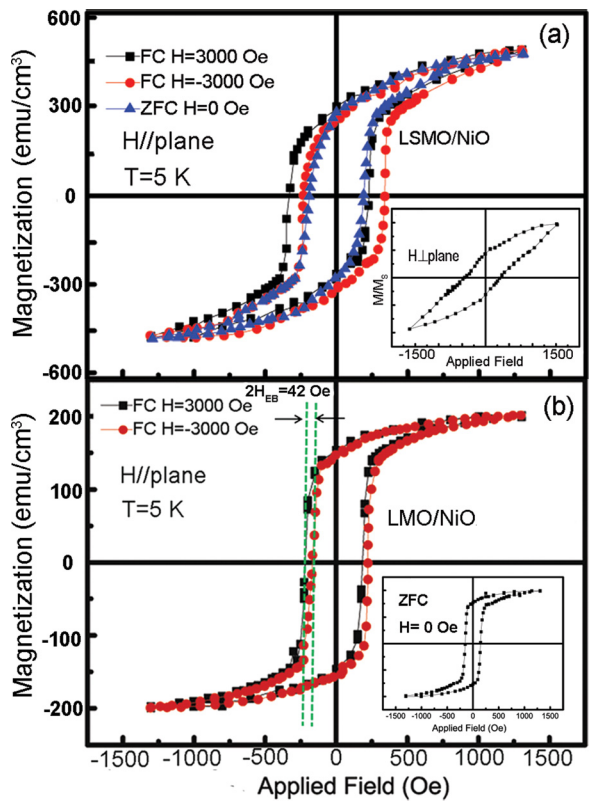

FIG. 4. (a) Magnetic hysteresis loops of LSMO/NiO bilayer at 5 K after ZFC and FC. Magnetization is normalized by the saturated value. Insert: the curve measured after cooling under an out-of-plane H_{FC} (= ± 3000 Oe). (b) Magnetic hysteresis loops of LMO/NiO bilayer after field cooling. Insert: the magnetic hysteresis loop after zero field cooling.

Even if the EB effect in these bilayers is understood as induced uncompensated spins, it is still not clear why a substantial difference in H_{EB} exists between the two systems. We looked into the band characters based on the Anderson exchange theory and the Anderson-Goodenough-Kanamori rule,[25,26] in which the FM exchange strength is evaluated by $E \propto |b_{(Mn,Ni)}|^2/U_{(Mn,Ni)}$, with b the transfer integral and $U_{(Mn,Ni)}$ the Hubbard parameter U of the d-electron for Ni and Mn. The Hubbard parameter U in LMO, which is large (= 4 eV, Ref. 8) because the d-d splitting in LMO is predominantly of purely electrostatic origin other than due to the 3d-2p hybridization,[24] is not expected to be substantially different from U in the LSMO. The transfer integral b might play a more substantial role and differences between the two systems can be seen from spin configuration analysis. Double-exchange requires ferromagnetic alignment of spins between neighboring ions at the interface,[25,27] such as between Mn^{3+} (or Mn^{4+}) and Ni^{2+}, but the ability of the electron to hop from Ni^{2+} to Mn^{3+} and Mn^{4+} differs. A higher hopping probability is anticipated between Ni^{2+} and Mn^{4+} than between Mn^{3+} and Ni^{2+}, which therefore gives rise to a bigger b in LSMO than in LMO films. In contrast, in LMO, the ground configuration of Mn^{3+} is $(t_{2g})^3(e_g)^1$ which gives rise to a high spin ground state. Comparing the doping FM conductor LSMO, including the effect of the inequivalent sites occupied by Mn^{4+} ions, we interpret the different EB effects in these samples to reflect the relationship between the Mn spin state (energy level) and the interfacial covalent bonding strength. That is to say, according to the simple superexchange rules, the magnetic interaction between Mn^{4+} and Ni^{2+} at the interface is FM.[27] Taking into account the facts above, we can speculate that the different energy competing processes and the states of the ions at the interface should play an important role in the interfacial exchange coupling.

To further understand the different magnetic interactions between the LSMO/NiO and LMO/NiO, the chemical valence states of the elements at the interface have been studied by X-ray photoelectron spectroscopy (Fig. 5). The Mn 3*s* and Ni 2*p* core-level spectra of the LSMO/NiO and LMO/NiO films have been used to analyze the Mn and Ni valence states. Figure 5(a) shows different splitting magnitudes in the binding energy of Mn 3*s* for the two samples. This energy separation magnitude is derived from the different valence states of the Mn ions due to the interaction between the 3*s* core hole and 3*d* electrons for the 3*d* transition metals.[28,29] A direct experimental result is that the energy separation (ΔE) between the splitting peaks of 3*S*(1) and 3*S*(2) is about $\Delta E \sim 5.06 \pm 0.1$ eV and ~5.45 ± 0.1 eV for LSMO/NiO and LMO/NiO bilayers, respectively. The XPS spectra were measured after etching times from 0 s to 210 s, and ΔE

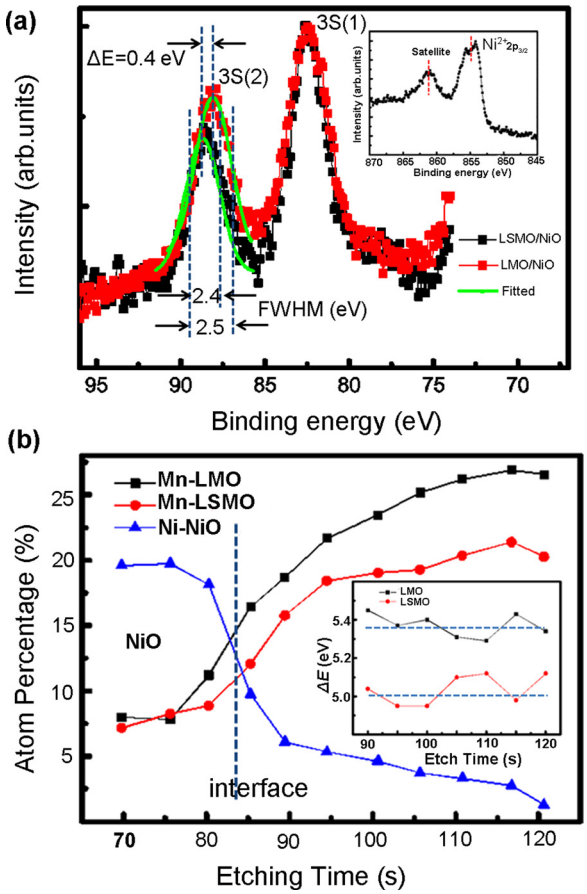

FIG. 5. (a) Mn 3*s* core-level XPS spectra of LSMO/NiO and LMO/NiO. Insert: Ni 2*p* core-level XPS spectra of LSMO/NiO. (b) The detailed information of atom percentage of the LSMO/NiO and LMO/NiO bilayers at different etching time. Insert: Separated energy (ΔE) of the LSMO and LMO films measured from 90 s to 120 s (from the interface to the internal of the films).

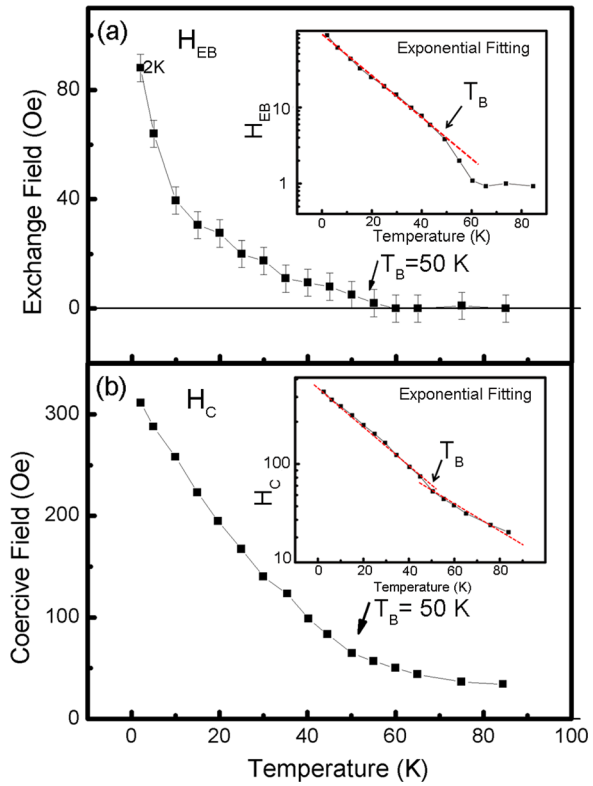

FIG. 6. (a) Exchange-bias field H_{EB} and (b) coercivity H_C of LSMO/NiO bilayer as a function of temperature (from 2 K to 85 K). Insert: Exponential fitting of the exchange bias field H_{EB} and coercivity H_C as a function of temperature.

did not change much from the surface to the inner LSMO and LMO films (Fig. 5(b)). The values are in good agreement with $\Delta E \sim 5.5$ eV (Mn^{3+}) and 4.5 eV (Mn^{4+}) reported by Wu *et al.*[29] The XPS results show that Mn ions are mainly in +3 state at the interface of LMO/NiO, but in the +3/+4 states at the interface of LSMO/NiO. However, May *et al.* pointed out that the weak tendency of Mn^{3+} to become Mn^{4+} in a LMO thin film can induce an FM phase.[15]

Furthermore, experimentally, the Ni 2*p* spectra (inset of Fig. 5(a)) show no obvious change for the two films (a direct detection of Ni^{3+} is difficult because of the metallic Ni during sputtering; here, we show one of these). We can speculate that the FM interaction between Ni^{2+} and Mn^{4+} is a favorable response to the interfacial EB effect.[30] If this is the case, this EB effect is stable against the applied field direction. Thus, a similar EB field is observed when the cooling fields and the measuring fields were applied along the out-of-plane direction for the LSMO/NiO sample (inset in Fig. 4(a)). In addition, also note that the relative value of the full width at half maximum (FWHM) and the intensity of the 3S(2) component were enhanced in the LSMO/NiO samples (Fig. 5). This value is affected by ligand chemistry and correlated with charge transfer between the Mn 3*d* and the ligand *p* states.[31,32] The decrease in charge transfer from 2*p* to 3*d* can increase the core-level 3*s* spectra ratio due to screening effects as well as the residual spin states on the *p* and *d* orbitals.[31] Thus, the p-d hybridization strength or the transfer integral *b* increases across the LSMO/NiO interface.

Having established this, we now turn to the temperature dependence of the exchange field H_{EB} of the LSMO/NiO bilayer. We measured the hysteresis loops at each temperature after FC from 340 K. Figure 6 shows the temperature variation of the H_{EB} and H_C from 2 K to 85 K for the LSMO/NiO bilayer. H_{EB} decreases almost monotonically with increasing temperature and vanishes at about 50 K, corresponding to conventional EB-blocking temperature T_B. Similarly, from Fig. 6(b), H_C decreases monotonically with increasing temperature. If seen on a logarithmic scale (insets of Fig. 6), H_{EB} and H_C decay exponentially with temperature with H_C, in particular, showing a crossover at T_B. In addition, the enhancement of the H_{EB} and H_C with lowering temperature seems to follow the conventional EB, which has been observed in FM/AFM structures.[33] It is known that the coercive field is determined by the density of Ni^{2+}-Mn^{4+} pairs, and the pinned uncompensated spin strengthens with lowering temperature.

IV. CONCLUSIONS

We have grown $La_{0.7}Sr_{0.3}MnO_3$/NiO and $LaMnO_3$/NiO bilayers and found an unconventional EB effect in these bilayer structures. The absolute values of the EB field H_{EB} and coercivity field H_C monotonically decrease with

increasing temperature. The large Hubbard parameter U and small transfer integral b can result in a weaker FM coupling effect at the LMO/NiO than at the LSMO/NiO interface. The XPS result shows the detailed valence of the Mn and Ni ions. The FM interaction between Ni^{2+} and Mn^{4+} is important for this unconventional EB effect in the LSMO/NiO and LMO/NiO bilayers.

ACKNOWLEDGMENTS

We gratefully acknowledge the partial support of this work by the Hundred Talents Program of the Chinese Academy of Sciences, the National Natural Science Foundation of China (Nos. 51072202 and 51172238) and the National Basic Research Program (No. 2010CB934603) of China, Ministry of Science and Technology, China.

[1]J. Hérault, R. C. Sousa, C. Ducruet, B. Dieny, Y. Conraux, C. Portemont, K. Mackay, I. L. Prejbeanu, B. Delaët, M. C. Cyrille, and O. Redon, J. Appl. Phys. **106**, 014505 (2009).
[2]P. K. Muduli and R. C. Budhani, J. Appl. Phys. **106**, 103924 (2009).
[3]C. T. Chao, C. Y. Kuo, L. Horng, M. Tsunoda, M. Takahashi, and J. C. Wu, J. Appl. Phys. **111**, 07B103 (2012).
[4]W. H. Meiklejohn and C. P. Bean, Phys. Rev. **105**, 904 (1957).
[5]X. Ke, L. J. Belenky, C. B. Eom, and M. S. Rzchowski, J. Appl. Phys. **97**, 10K115 (2005).
[6]Y. Lee, B. Caes, and B. N. Harmon, J. Alloys Compd. **450**, 1 (2008).
[7]J. C. Rojas Sánchez, B. Nelson-Cheeseman, M. Granada, E. Arenholz, and L. B. Steren, Phys. Rev. B **85**, 094427 (2012).
[8]M. Gilbert, P. Zubko, R. Scherwitzl, J. Iniguez, and J. M. Triscone, Nature Mater. **11**, 195 (2012).
[9]S. J. Zhu, J. Yuan, B. Y. Zhu, F. C. Zhang, B. Xu, L. X. Cao, X. G. Qiu, B. R. Zhao, and P. X. Zhang, Appl. Phys. Lett. **90**, 112502 (2007).
[10]K. D. Sung, Y. A. Park, M. S. Seo, Y. Jo, N. Hur, and J. H. Jung, J. Appl. Phys. **112**, 033915 (2012).
[11]A. Gupta, T. R. McGuire, P. R. Duncombe, M. Rupp, J. Z. Sun, and W. J. Gallagher, Appl. Phys. Lett. **67**, 3494 (1995).
[12]T. Saitoh, A. E. Bocquet, T. Mizokawa, H. Namatame, A. Fujimori, M. Abbate, Y. Takeda, and M. Takano, Phys. Rev. B **51**, 13942 (1995).
[13]S. Dong, R. Yu, S. Yunoki, G. Alvarez, J. M. Liu, and E. Dagotto, Phys. Rev. B **78**, 201102(R) (2008).
[14]A. Kleine, Y. Luo, and K. Samwer, Europhys. Lett. **76**, 135 (2006).
[15]A. Bhattacharya, S. J. May, S. G. E. te Velthuis, M. Warusawithana, X. Zhai, B. Jiang, J. M. Zuo, M. R. Fitzsimmons, S. D. Bader, and J. N. Eckstein, Phys. Rev. Lett. **100**, 257203 (2008).
[16]M. Takahara, H. Jinn, S. Wakabayashi, T. Moriyasu, and T. Kohmoto, Phys. Rev. B **86**, 094301 (2012).
[17]W. S. Choi, D. W. Jeong, S. Y. Jang, Z. Marton, S. S. A. Seo, H. N. Lee, and Y. S. Lee, J. Korean Phys. Soc. **58**, 569 (2011).
[18]N. H. March, P. Lambin, and F. Herman, J. Magn. Magn. Mater. **44**, 1 (1984).
[19]M. G. Blamire, IEEE Trans. Magn. **44**, 1946 (2008).
[20]J. W. Cai, K. Liu, and C. L. Chien, Phys. Rev. B **60**, 72 (1999).
[21]K. D. Sossmeier, L. G. Pereira, J. E. Schmidt, and J. Geshev, J. Appl. Phys. **109**, 083938 (2011).
[22]D. Lebeugle, A. Mougin, M. Viret, D. Colson, J. Allibe, H. Béa, E. Jacquet, C. Deranlot, M. Bibes, and A. Barthélémy, Phys. Rev. B **81**, 134411 (2010).
[23]P. Yu, J.-S. Lee, S. Okamoto, M. D. Rossell, M. Huijben, C.-H. Yang, Q. He, J. X. Zhang, S. Y. Yang, M. J. Lee, Q. M. Ramasse, R. Erni, Y.-H. Chu, D. A. Arena, C.-C. Kao, L. W. Martin, and R. Ramesh, Phys. Rev. Lett. **105**, 027201 (2010).
[24]R. J. Radwanski and Z. Ropka, J. Phys.: Conf. Ser. **303**, 012116 (2011).
[25]P. W. Anderson, Phys. Rev. **115**, 2 (1959).
[26]J. B. Goodenough, Phys. Rev. **100**, 564 (1955).
[27]B. Kim, J. Lee, B. Hyun Kim, H. C. Choi, K. Kim, J.-S. Kang, and B. I. Min, J. Appl. Phys. **105**, 07E515 (2009).
[28]V. A. M. Brabers, F. M. Van Setten, and P. S. A. Knapen, J. Solid State Chem. **49**, 93 (1983).
[29]Q. H. Wu, M. L. Liu, and W. Jaegermann, Mater. Lett. **59**, 1980 (2005).
[30]D. Choudhury, P. Mandal, R. Mathieu, A. Hazarika, S. Rajan, A. Sundaresan, U. V. Waghmare, R. Knut, O. Karis, P. Nordblad, and D. D. Sarma, Phys. Rev. Lett. **108**, 127201 (2012).
[31]A. J. Nelson, J. G. Reynolds, and G. Christou, J. Appl. Phys. **93**, 2536 (2003).
[32]M. Fujiwara, T. Matsushita, and S. Ikeda, J. Electron Spectrosc. Relat. Phenom. **74**, 201 (1995).
[33]C. Prados, E. Pina, A. Hernando, and A. Montone, J. Phys.:Condens. Matter **14**, 10063 (2002).